HHS Public Access

Author manuscript

Bioconjug Chem. Author manuscript; available in PMC 2018 April 18.

Published in final edited form as:

Bioconjug Chem. 2017 October 18; 28(10): 2581–2590. doi:10.1021/acs.bioconjchem.7b00418.

Dynamic Equilibrium of cTnC's Hydrophobic Cleft and Its Modulation by Ca^{2+} Sensitizers and a Ca^{2+} Sensitivity blunting phosphomimic, cTnT(T204E)

William Schlecht[1] and **Wen-Ji Dong**[1,2]

[1]The Voiland School of Chemical Engineering and Bioengineering, Washington State University, Pullman, Washington 99164, USA

[2]The Department of Integrated Neuroscience and Physiology, Washington State University, Pullman, Washington 99164, USA

Abstract

Several studies have suggested that conformational dynamics are important in cardiac troponin C's (cTnC's) regulation of thin filament activation, however little direct evidence has been offered to support these claims. In this study, a dye homodimerization approach is developed and implemented which allows for determination of the dynamic equilibrium between open and closed conformations in cTnC's hydrophobic cleft. Modulation of this equilibrium by Ca^{2+}, cardiac troponin I (cTnI), cardiac troponin T (cTnT), Ca^{2+}-sensitizers, and a Ca^{2+} desensitizing phosphomimic of cTnT (cTnT(T204E) is characterized. Isolated cTnC contained a small open conformation population in the absence of Ca^{2+}, which increased significantly upon addition of saturating levels of Ca^{2+}. This suggests the Ca^{2+} induced activation of thin filament arises from an increase in the probability of hydrophobic cleft opening. Inclusion of cTnI increased the population of open cTnC while inclusion of cTnT had the opposite effect. Samples containing Ca^{2+}-desensitizing cTnT(T204E) showed a slight but insignificant decrease in open conformation probability compared to samples with cTnT(wt), while Ca^{2+}-sensitizer treated samples generally increased open conformation probability. These findings show that an equilibrium between open and closed conformations of cTnC's hydrophobic cleft are play a significant role in tuning the Ca^{2+} sensitivity of the heart.

Graphical Abstract

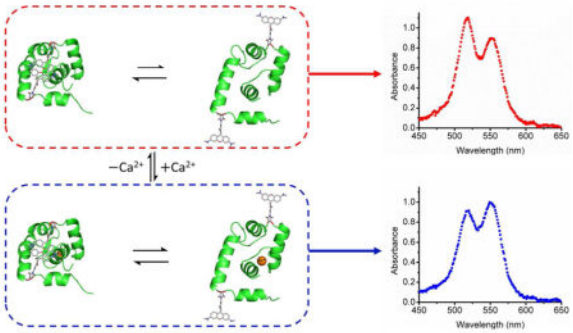

Introduction

The cardiac troponin complex (cTn) transduces the sarcomeric Ca^{2+} transient into the cyclic contraction and relaxation of the myocardium responsible for pumping blood throughout the body. A hetero-trimeric protein, cTn consists of troponin I which inhibits force generation, troponin C which binds Ca^{2+} and removes cTnI's inhibition of force, and troponin T which tethers this cTn to tropomyosin and actin. When sarcomeric Ca^{2+} concentrations are low cTn in conjunction with tropomyosin inhibits the strong actin-myosin binding required for force generation. As the Ca^{2+} concentration within the sarcomere increases this inhibition is released and force generation begins. The troponin subunit responsible for releasing cTnI's inhibition in a Ca^{2+} dependent manner is cTnC, which possesses a single regulatory Ca^{2+} binding site within its N-terminal half (known as site II). When Ca^{2+} binds to this site cTnC's helices B and C move away from helices N, A, and D increasing the exposure of hydrophobic residues, known as the hydrophobic cleft, to which cTnI's regulatory region (cTnI residues 150–165) can bind. As cTnI's regulatory region binds cTnC's hydrophobic cleft, the inhibitory region of cTnI (cTnI residues 130–149) is pulled away from actin's surface allowing myosin to strongly bind actin. This, in conjunction with tropomyosin movement away from myosin binding sites on actin, enables the strong actin-myosin interaction which generates force.[1] Thus, the events leading to cardiac contraction represent a tightly coupled cascade of structural transitions beginning with Ca^{2+} binding to cTnC and proceeding through to strong actin-myosin binding. This illustrates the central role cTnC has in regulating cardiac contraction and explains why mutations or pharmaceuticals which alter cTnC function have a large impact on cardiac contractility.[2–5] But despite its importance and the many studies focused on it cTnC has yet to be fully characterized. In particular, the role dynamic conformational equilibria play in cTnC's regulation of cardiac contraction has yet to be satisfactorily explored.

In recent years the essential role of conformational dynamics in protein function has become increasingly clear. The current view is that most allosteric proteins exist in dynamic equilibrium between various physiologically relevant conformations.[6–7] Thus, to fully understand how a protein functions it is necessary to characterize the structure and function of all accessible conformations, the equilibrium between these conformations, and how ligand binding alters this equilibrium. An increasing body of evidence suggests cTnC exists in dynamic conformational equilibrium and that Ca^{2+} binding regulates this equilibrium.[8–10] However, the current literature on cTnC's dynamic equilibria disagree regarding two key points. The first is if Ca^{2+} binding to site II causes uniform adoption of an ajar, "primed-closed", conformation wherein cTnC's hydrophobic cleft is partially open, or if this seemingly ajar conformation is in fact a dynamic equilibrium between fully open and closed states of cTnC's hydrophobic cleft. The second is whether cTnI's regulatory region binds with cTnC's hydrophobic cleft via an induced fit to the primed-closed conformation or by a population shift mechanism where the regulatory region selectively binds to cTnC while it samples the fully open conformation. The present study seeks to settle these disagreements while also investigating how cTnC's dynamic conformational equilibria are modulated by the presence of cTnI, cTnT, Ca^{2+} sensitizers, or Ca^{2+} desensitizing mutations/post-translational modifications.

The current study develops and employs a TAMRA labeling scheme capable of determining the fractional abundance of open and closed conformations of cTnC's hydrophobic cleft. Briefly, TAMRA molecules are conjugated to residues 13C and 51C in mutant cTnC, these residues residing on opposite sides of the hydrophobic cleft. This double TAMRA labeled cTnC mutant is henceforth referred to as cTnC(13C/51C)$_{TAMRA2}$. When cTnC's hydrophobic cleft is closed (or ajar) the two TAMRA molecules will associate and form a TAMRA dimer which has a unique absorbance spectrum. When the hydrophobic cleft is fully open the two TAMRA molecules are unable to interact and no dimer forms, the absorbance spectra observed in this case is that of pure monomeric TAMRA.[11] Thus, dynamic equilibria between open and closed/primed-closed conformations of the hydrophobic cleft can be determined from the relative abundance of monomeric and dimeric TAMRA, which can in turn be determined from the measured absorbance spectra.

Absorbance spectra measurements were carried out in the presence and absence of Ca^{2+} for cTnC(13C/51C)$_{TAMRA2}$, cTnI(wt)-cTnC(13C/51C)$_{TAMRA2}$, cTnI(wt)-cTnC(13C/51C)$_{TAMRA2}$-cTnT(wt), and cTnI-cTnC(13C/51C)$_{TAMRA2}$-cTnT(T204E), where cTnT(T204E) is a known Ca^{2+} desensitizing phosphorylation mimic. Additionally, each of these treatments was conducted in the presence of either bepridil, levosimendan, or pimobendan, three well known Ca^{2+} sensitizers. The results show isolated cTnC contains an equilibrium between monomeric and dimeric TAMRA in both the presence and absence of Ca^{2+}, implying a dynamic equilibrium between open and closed conformations of the hydrophobic cleft. This equilibrium was modulated by Ca^{2+} binding which served to increase the population of TAMRA monomer/open cTnC from approximately 14.5% to 33.9%. This finding supports the hypothesis that Ca^{2+} binding to cTnC regulates force generation by shifting the dynamic equilibrium of the hydrophobic cleft towards open conformations. The relatively large increase in hydrophobic cleft opening probability induced by Ca^{2+} binding suggests conformational selection is the mechanism by which cTnI's regulatory region binds the hydrophobic cleft of cTnC, however, the methods of the present study are not able to fully rule out an induced fit mechanism. Samples containing cTnI showed significantly reduced abundance of dimeric TAMRA in the absence of Ca^{2+}, an effect mostly attributed to steric clash between the regulatory region of cTnI with TAMRA. Samples containing cTnI in the presence of saturating Ca^{2+} showed a significant increase in TAMRA monomer/open cTnC consistent with the notion that cTnI binding stabilizes the open conformation of cTnC. Inclusion of cTnT reduced the amount of cTnI-dimer clash in the absence of Ca^{2+}, most likely by decreasing the mobility of cTnI via the stabilizing effect of the IT arm. The Ca^{2+} desensitizing phosphorylation mimic, cTnT(T204E), appears to further reduce the cTnI-dimer clash, suggesting a reduced collisional rate between cTnI's regulatory region and cTnC may explain how cTnT(T204E) is able to reduce Ca^{2+} sensitivity of the troponin complex. Addition of Ca^{2+} sensitizing agents increased the TAMRA monomer/open population in cTnC in both the presence and absence of Ca^{2+}, consistent with the view that these drugs stabilize the open conformation of cTnC. All sensitizers tested had a stronger effect on cTnC's dynamic equilibrium in the presence of Ca^{2+} or cTnI. This suggests both Ca^{2+} and cTnI enhance sensitizers binding to cTnC. Taken together, the results of this study show that dynamic equilibria in cTnC and the modulation

thereof by cTnI(wt), cTnT(wt) and cTnT(T204E), and Ca^{2+} sensitizers are essential to understanding how cTnC regulates force generation in the heart.

Results and Discussion

The cTnC(T13C/N51C)$_{TAMRA2}$ labeling scheme, a binary reporter

The ability of TAMRA to form non-covalent homodimers is a well documented process.[12–14] When in close proximity TAMRA molecules readily form non-fluorescent homodimers by stacking of their xanthene rings. The dimer displays a hypsochromically shifted absorbance peak at 520 nm while monomeric TAMRA has a peak absorbance at 554 nm. By comparing the absorbance at 520 and 554 nm the relative abundance of monomeric and dimeric TAMRA can be found (see “Absorbance data processing” for more details). The process of TAMRA dimerization can be described by the reaction shown below.

$$D \underset{k_{-1}}{\overset{k_1}{\rightleftarrows}} M+M \quad 1)$$

The ratio of the forward and backward rate constants (k_1/k_{-1}) is known as the dissociation constant (K_d) and when the TAMRA concentration in solution is near or above this value, 1.37×10^{-4} M for TAMRA, the concentration of dimer becomes significant.[15] So long as the bulk concentration of TAMRA is well below the dissociation constant, as in the present study, the expected concentration of dimer is approximately zero. However, when two or more TAMRA molecules are labeled to the same protein, and the labeling sites are sufficiently close such that interaction between TAMRA’s xanthene rings can occur, intramolecular dimerization becomes possible.[12–14] For two TAMRA molecules attached via linkers of length R (14.36 Å in this case via molView) to residues within a single protein the probability of dimerization can be modeled as a function of the separation distance, d, between the labeled residues. To derive this model each TAMRA is considered to freely diffuse in a spherical shell with outer radius R (the maximum linker length) and inner radius r (the minimum linker length, approximately 9.36 Å in this case via molView) centered on the residue to which it is labeled. Thus, within this shell the concentration of TAMRA is given by equation 2, where V_{shell} is the volume of the spherical shell bounded by inner radius r and outer radius R.

$$\frac{1/\text{Avogadro's number}}{V_{shell}} \quad 2)$$

When the inter-residue separation distance, d, is sufficiently small such that overlap between the two shells occurs the volume of this overlap region is given by equation 3.

$$V_{overlap} = V_{RR} - 2V_{Rr} + V_{rr} \quad 3)$$

Where V_{RR} is the intersectional volume of two spheres with radii equal to R having centers separated by a distance d. V_{Rr} is the intersectional volume of two spheres separated by d where one of the spheres has a radius equal to the minimal linker length r, with the other sphere having a radius equal to the maximum linker length, R. Finally, V_{rr} is the intersectional volume of two spheres with radii equal to r separated by distance d. Each of these values can be calculated as a function of the separation distance, d, according to equation 4.

$$V_{Rr} = \frac{\pi (R + r - d)^2 (d^2 + 2dr - 3r^2 + 2dR + 6rR - 3R^2)}{12d} \quad 4)$$

The equations for V_{RR} and V_{rr} are simply cases of equation 4 where R and r both equal either the maximal (R) or minimal (r) linker length. The total TAMRA concentration within this overlap region is given by equation 5.

$$[TAMRA]_{Total} = \frac{2/Avogadro's\ Number}{V_{shell}} \quad 5)$$

And the total rate of dimer formation within this overlap region is given below.

$$k_{-1}[M]^2 V_{overlap} \quad 6)$$

Because our system consists of only two TAMRA molecules, if one of those molecules is in the monomer state the other must be as well. Thus, in our quantized system there are only two possible rates of dimerization, these are when both molecules of TAMRA are in the monomer state and thus [M] = $[TAMRA]_{total}$ or when both are in the dimer state and [M] = 0. So, for a large number of such systems the average rate of dimer formation is given by equation 7.

$$Rate_{Dimer\ Formation} = F(M) k_{-1} [TAMRA]_{total}^2 V_{overlap} \quad 7)$$

Where

$$F(M)=\frac{Number\ of\ systems\ in\ the\ monomer\ state}{Total\ number\ of\ systems} \quad 8)$$

The average rate of dissociation for the two TAMRA system can be found in a similar manner, however one key point is that when the system is in the dimer state both TAMRA molecules must be present somewhere in the overlap region. This means that when the system is in the dimer state the dimer concentration in the overlap region is that given in equation 9.

$$\frac{[\,TAMRA]_{Total}\left(\frac{V_{shell}}{V_{overlap}}\right)}{2} \quad 9)$$

Thus, within the quantized system the total rate of dimer dissociation is either 0 or

$$\frac{k_1[\,TAMRA]_{Total}\left(\frac{V_{shell}}{V_{overlap}}\right)V_{overlap}}{2}=\frac{k_1}{2}[\,TAMRA]_{Total}V_{shell} \quad 10)$$

As before the average rate of dissociation for many such systems is

$$Rate_{Dimer\ Dissociation}=F(D)\frac{k_1}{2}[\,TAMRA]_{Total}V_{shell} \quad 11)$$

Where

$$F(D)=\frac{Number\ of\ systems\ in\ the\ dimer\ state}{Total\ number\ of\ systems} \quad 12)$$

Having expressions for the average rates of dimerization and dissociation and knowing that at steady state these rates must equal, we set equations 7 and 11 equal to one another. Knowing that F(M) and F(D) must add to one, we can replace F(M) with 1-F(D). Solving for F(D) yields equation 13 (shown below), which gives the probability of TAMRA being in the dimer state as a function of separation distance between the two labeled residues.

$$F(D)=\frac{1}{1+\frac{K_d}{2[\,TAMRA]_{Total}}\frac{V_{shell}}{V_{overlap}}} \quad 13)$$

Although equation 13 was derived for the purposes of this study, the result is generally applicable to any case in which a protein or other substrate is double labeled with a dye capable of homodimerization and can be applied so long as the dissociation constant and linker structure is known. Plugging in the parameters for the specific case of cTnC(T13C/N51C)$_{TAMRA2}$ and plotting the probability of TAMRA dimerization as a function of 13C-51C separation distance gives figure 1.

As can be seen in figure 1. the probability of dimerization as a function of 13C-51C separation distance predicts binary behavior, with nearly 100% dimerization at distances less than 28.7 Å, and 0% dimerization for distances greater than this. This binary quality of the TAMRA labeling scheme informs interpretation of the following results. Because cTnC residues 13C and 51C lie on opposite sides of the hydrophobic cleft and because the distance between these residues is known to be approximately 21.7 Å in the absence of Ca^{2+} (closed conformation), 23.9 Å in the presence of Ca^{2+} (proposed primed-closed conformation), and 28.9 Å in the presence of both Ca^{2+} and cTnI (open conformation) we can equate dimeric TAMRA with the closed/primed-closed conformations (13C-51C distances less than 28.7 Å) and monomeric TAMRA with the open conformation (cTnC 13C-51C separation greater than 28.7 Å).[9, 16] If cTnC exists in conformational equilibrium between open and closed/prime-closed conformations this will appear as an equilibrium between monomeric and dimeric TAMRA species, with the relative abundance of monomeric and dimeric TAMRA corresponding to the relative abundance of the open and closed/primed-closed conformations respectively.

Absorbance spectra measurements

Absorbance spectra such as those shown in figure 2, were measured for cTnC(T13C/N51C)$_{TAMRA2}$, cTnI(wt)-cTnC(T13C/N51C)$_{TAMRA2}$, cTnI(wt)-cTnC(T13C/N51C)$_{TAMRA2}$-cTnT(wt), and cTnI(wt)-cTnC(T13C/N51C)-cTnT(T204E) in the presence or absence of saturating Ca^{2+}. Each of these treatments was then repeated in the presence of 100 μM levosimendan, pimobendan, or bepridil. All absorbance spectra were deconvoluted to give the fractional abundance of TAMRA in the monomeric and dimeric states, this data was analyzed via two-way ANOVA and Tukey's honest significant difference. These results are recorded in tables 1 and 2 below.

Conformational equilibrium in cTnC

The results recorded in table 1 show Mg^{2+}-cTnC(T13C/N51C)$_{TAMRA2}$ samples contain 85.5% TAMRA dimer. Put another way, at any given moment 85.5% of the Mg^{2+}-cTnC(T13C/N51C)$_{TAMRA2}$ molecules must be in a closed or primed-closed conformation in order for the xanthene rings of the two TAMRAs to be close enough to dimerize. The 14.5% of the Mg^{2+}-cTnC(T13C/N51C)$_{TAMRA2}$ population which contains TAMRA monomers must be in an open conformation. This suggests cTnC is never fully deactivated even in the absence of Ca^{2+}. Although the notion of incomplete deactivation of cTnC has been proposed in various studies, this is the first time it has been observed directly.[9, 17–18] A previous NMR study suggested that if an open population exists in Mg^{2+}-cTnC that this population must be less than 15%, which is in agreement with our value of 14.5%. Upon addition of saturating Ca^{2+} to cTnC (see table 2) the TAMRA dimer population is reduced to 66.1% (monomer

abundance increased to 33.9%), thus Ca^{2+} induces a significant 19.4% decrease in the closed population of cTnC even in the absence of cTnI and cTnT. This illustrates that Ca^{2+} binding alone is sufficient induce full opening (even if transient) of cTnC's hydrophobic cleft. Our value of 33.9% opening in Ca^{2+}-cTnC(T13C/N51C)$_{TAMRA2}$ is in reasonable agreement with the study by Cordina et al. which showed approximately 27% opening in Ca^{2+}-cTnC.[8] These results refute the idea that Ca^{2+} binding to cTnC causes uniform adoption of the primed-closed conformation in which cTnC's hydrophobic cleft is only slightly ajar (13C-51C separation distance of 23.9 Å) because adoption of this conformation would be insufficient to induce significant changes in TAMRA's probability of dimerization (see figure 1). Based on these results, it is proposed that Ca^{2+} binding to isolated cTnC substantially increases the probability of full opening of the hydrophobic cleft, and that cTnI's regulatory region selectively binds to the transiently open conformation of cTnC's hydrophobic cleft (population shift). Despite a population shift mechanism being suggested by these results, the present study is not able to fully rule out an induced fit mechanism, and further study is recommended.

Effect of cTnI on cTnC's conformational equilibrium

Looking at table 1 row 2, it can be seen that the TAMRA dimer population in Mg^{2+}-cTnI(wt)-cTnC(T13C/N51C)$_{TAMRA2}$ is significantly reduced compared to Mg^{2+}- (42.4% compared to 85.5%). This drastic reduction in dimer cTnC(T13C/N51C)$_{TAMRA2}$ population likely results from two main causes. First, steric clash of cTnI with dimerized TAMRA molecules would disrupt dimer formation. Because the regulatory region of cTnI interacts directly with the hydrophobic cleft of cTnC it must pass through the region where the TAMRA dimer forms. Thus, the relatively mobile cTnI can interfere with TAMRA dimer formation and reduce the dimer population without subsequent changes in cTnC's structure. The second possible cause is a shift in the conformational equilibrium in cTnC induced by the presence of cTnI either through direct binding to cTnC's hydrophobic cleft or via alteration in the relative stabilities of cTnC's closed and open conformations. Unfortunately, the approach used in this study is unable to directly determine the contributions of each effect. However, by comparing our results to FRET distance measurements taken in a previous study by Robinson et al. we can obtain some insight.[9] In our study, addition of saturating Ca^{2+} to cTnC induces a 19.4% increase in TAMRA monomer, in Robinson's study this same transition resulted in a 2.2 Å increase in distance between the labeled residues 12 and 51 in cTnC, thus we obtain a conversion factor of 8.82 %/Å with which we can convert between FRET distance change and expected TAMRA population change. In Robinson's study addition of cTnI to Mg^{2+} -cTnC caused a relatively small 0.6 Å increase in FRET distance, using our conversion factor we would expect a 5.3% increase in the monomer population. Our data however shows an increase of 43.1% in the monomer population. Obviously addition of cTnI to Mg^{2+}-cTnC(T13C/N51C)$_{TAMRA2}$ has a much larger impact on the TAMRA dimer/monomer equilibrium than would be expected based on FRET structural data. This discrepancy between our results and FRET structural results is explained by the fact that FRET distance values will be unaffected by steric clash with cTnI, while TAMRA dimerization will be inhibited by the presence of cTnI. We suggest that Mg^{2+} -cTnI(wt)-cTnC(T13C/N51C)$_{TAMRA2}$ most likely exists in the closed conformation approximately 80.2% of the time, but that steric clash with cTnI reduces the TAMRA dimer

population by an additional 37.8%. Finally, according to Robinson's FRET structural data the addition of Ca^{2+} and cTnI causes between a 6.6 Å – 7.2 Å opening in cTnC's hydrophobic cleft, using our conversion factor this corresponds to an expected dimer population in Ca^{2+}-cTnI(wt)-cTnC(T13C/N51C)$_{TAMRA2}$ of 27.3% - 22.0% which is in good agreement with our measured dimer population of 31.3% (see table 2). This implies that Ca^{2+}-cTnI(wt)-cTnC(T13C/N51C)$_{TAMRA2}$ does not suffer from significant steric clash induced dimer disruption. This makes sense because in the presence of Ca^{2+} cTnI will spend much of its time bound to cTnC, greatly reducing probability of a cTnI collision with TAMRA dimer. In summary, we suggest Ca^{2+} induces an approximate 48.9% increase in the open conformation of cTnC when in the presence of cTnI going from approximately 80.2% dimer in the Mg^{2+} state to 31.3% dimer in the Ca^{2+} state.

Effect of cTnT and cTnT(T204E) on cTnC's conformational equilibrium

As recorded in table 1 rows 3 and 4, on average, samples containing cTnT(wt) or cTnT(T204E) in the Mg^{2+} state possessed a larger dimer population than Mg^{2+}-cTnI(wt)-cTnC(T13C/N51C)$_{TAMRA2}$ samples. This trend persists in the presence of Ca^{2+} as can be seen by looking at table 2 rows 3 and 4, wherein it can be observed that addition of either cTnT(wt) or cTnT(T204E) to Ca^{2+}-cTnI(wt)-cTnC(T13C/N51C)$_{TAMRA2}$ caused an increase in cTnC's dimer population, however, this shift was smaller than that observed in the Mg^{2+} state. From FRET distance measurements between residues 13 and 51 in cTnC we do not see significant structural changes in the hydrophobic cleft induced by cTnT in the Mg^{2+} state, which implies cTnT is not altering cTnC structure or equilibrium, but is instead affecting cTnI's rate of collision with cTnC and thereby the TAMRA dimer.[9, 16] Thus, we conclude that cTnT(wt) and cTnT(T204E) increase the TAMRA dimer population in cTnC by reducing the ability of cTnI to collide with cTnC. The reason cTnT(wt) and cTnT(T204E) increase dimer population more in the Mg^{2+} state than in the Ca^{2+} state is because the Mg^{2+} state suffers from significant steric clash induced dimer disruption while the Ca^{2+} state does not, and since cTnT appears to reduce this steric clash it will naturally have a larger effect in the Mg^{2+} state than in the Ca^{2+} state. The reduced collisional rate of cTnI with cTnC in the presence of cTnT likely results from formation of the IT arm, a rigid structure which spatially restricts cTnI's movements.

Reduction in the rate of collision between cTnI's regulatory region and cTnC's hydrophobic cleft might be thought to reduce the Ca^{2+} sensitivity of cTnC, however Ca^{2+} titrations from a previous study show an increase in Ca^{2+} sensitivity instead of a reduction upon addition of cTnT(wt).[2] The most likely explanation, although no direct evidence for this is obtained in the present study, is that cTnT scaffolds cTnI via the IT arm which reduces the rate of collision between cTnI and cTnC while simultaneously increasing the population of cTnI bound to cTnC, either by causing cTnI to collide with cTnC in a more optimum orientation for binding, or by reducing the rate of cTnI dissociation from cTnC's hydrophobic cleft once bound. Thus, even though there are less collisions between cTnI and cTnC in the presence of cTnT the total probability of cTnI being bound to cTnC remains about the same or even increases.

In the absence of Ca^{2+}, samples containing cTnT(T204E), a known Ca^{2+} desensitizing phosphorylation mimic, contain more TAMRA dimer than samples containing cTnT(wt) (although this trend is not significant at the 0.05 level). Thus, it appears that cTnT(T204E)'s ability to reduce the collisional rate between cTnI and cTnC is even greater than that of cTnT(wt). As was the case with cTnT(wt), a reduction in collisional rate between cTnI and cTnC by itself would be expected to reduce the Ca^{2+} sensitivity of the troponin complex. In the case of cTnT(wt) this effect is likely mitigated by improvement in the collisional orientation of cTnI and cTnC, or by reduction in the rate of dissociation of cTnI from cTnC once bound, however for cTnT(T204E) it is unlikely that a further improvement in cTnI cTnC binding would occur via either of these mechanisms. Thus, we propose that the Ca^{2+} desensitization of the troponin complex induced by cTnT(T204E) occurs at least partially from a reduction in the rate of collision between cTnI and cTnC.[3, 19]

Based on these results it is hypothesized that incorporation of Mg^{2+}-cTnI(wt)-cTnC(T13C/N51C)$_{TAMRA2}$ or Mg^{2+}-cTnI(wt)-cTnC(T13C/N51C)$_{TAMRA2}$-cTnT(wt or T204E) into thin filaments (or more complex systems) would result in a substantial increase in their TAMRA dimer populations as compared to the results in this study. This is because actin (which composes thin filaments) is known to bind with, and reduce the mobility of, cTnI's regulatory region in the absence of Ca^{2+}. Thus, in the absence of Ca^{2+}, actin would be expected to greatly reduce steric clash between cTnI's regulatory region and cTnC(T13C/N51C)$_{TAMRA2}$'s TAMRA dimers, subsequently increasing the observed dimer population. This effect would be similar to what was observed in this study upon inclusion of cTnT(wt) and cTnT(T204E). It is also possible that addition of actin to Ca^{2+}-cTnI(wt)-cTnC(T13C/N51C)$_{TAMRA2}$ or Ca^{2+}-cTnI(wt)-cTnC(T13C/N51C)$_{TAMRA2}$-cTnT(wt or T204E) would reduce the amount of cTnC(T13C/N51C)$_{TAMRA2}$ opening since actin would compete with the hydrophobic cleft for binding to cTnI's regulatory region, however, this expectation is less certain.

Modulation of cTnC's dynamic equilibria by Ca^{2+} sensitizers

The difference in dimer abundance between vehicle and drug treated samples at the same reconstitution level provides a convenient way to quantify the impact each sensitizer has on cTnC's dynamic equilibrium. This difference is represented mathematically below in equation 14.

$$\text{Difference in dimer population} = D\%_{\text{vehicle}} - (F_{\text{unbound}} D\%_{\text{vehicle}} + F_{\text{bound}} D\%_{\text{drug}}) \quad 14)$$

Where F_{bound} and $F_{unbound}$ represent the fractions of drug bound and unbound cTnC respectively and $D\%_{vehicle}$ and $D\%_{drug}$ represent the equilibrium population of dimeric TAMRA in the absence of drug bound cTnC and in the presence of fully drug bound cTnC. This expression can be simplified to the following.

$$\text{Difference in dimer population} = F_{\text{bound}} (D\%_{\text{vehicle}} - D\%_{\text{drug}}) \quad 15)$$

The above expression makes it clear that the difference in dimer population between vehicle and drug treated samples depends both on the degree of drug binding as well as the extent to which the drug reduces the dimer population relative to drug unbound cTnC. It should be noted that a reduction in the dimer population in the vehicle sample will result in a reduction in the observed difference between drug treated and untreated samples, even if the behavior of the drug remains the same, a point we will return to shortly.

Tables 3 and 4 show the difference in dimer abundance between vehicle and drug treated samples at each level of reconstitution. As can be seen, all calcium sensitizer containing samples showed reduced dimer abundance at all levels of reconstitution in both the presence and absence of Ca^{2+}. This implies all sensitizers tested in this study work by shifting the dynamic equilibrium of cTnC towards the fully open conformation, which possesses higher Ca^{2+} affinity than closed cTnC.[9, 20] Despite this common mechanism of action each sensitizer showed distinct behavior which will be discussed in depth below.

Levosimendan showed almost no impact on the dimer population of Mg^{2+}-cTnC, but showed significant dimer population reduction in the presence of cTnI and/or Ca^{2+}. These results imply levosimendan is unable to substantially bind with cTnC in the absence of Ca^{2+} and cTnI at the concentrations tested, likely because the probability of hydrophobic cleft opening is too low. This agrees with an NMR study which showed the presence of Ca^{2+} was necessary for levosimendan to substantially bind with cTnC, the authors suggested that insufficient opening of the hydrophobic cleft limits levosimendan's ability to bind.[21] Accordingly, we propose that when the probability of hydrophobic cleft opening is increased, either by cTnC binding with Ca^{2+} or cTnI, levosimendan is able to induce a greater effect on the dynamic equilibrium in cTnC, as was observed in the present study. Thus, levosimendan appears to amplify the extent of cTnC opening induced by Ca^{2+} or cTnI binding.

Of the three Ca^{2+} sensitizers tested, bepridil induced the least significant reduction in dimer probability. Although bepridil displays a slightly larger impact on dimer population in the presence of cTnI, this increase is significantly smaller than that seen for levosimendan. This is most likely because bepridil competes with cTnI for binding to cTnC's hydrophobic cleft, as has been shown by previous studies.[22] As seen with levosimendan, bepridil also has a significantly larger impact on cTnC's dynamic equilibrium in the presence of Ca^{2+}, this is attributed to Ca^{2+} increasing exposure of the hydrophobic cleft, the region into which bepridil is known to bind.[5, 23–24] Essentially, bepridil displays the same binding behavior as levosimendan, that is, enhanced impact on cTnC's dynamic equilibrium in the presence of Ca^{2+} and (to a lesser extent) cTnI.

Pimobendan induced dramatic reduction in cTnC's dimer population at all levels of reconstitution in both the presence and absence of Ca^{2+}. However, a quick inspection of the results listed in tables 3 and 4 reveals the impact of pimobendan on cTnC's dynamic equilibrium appears to decrease in the presence of cTnI and Ca^{2+}, the opposite of what was observed for levosimendan and bepridil. Recalling equation 15, in the case that drug binding induces nearly full opening of cTnC ($D\%_{drug} = 0$) then the observed difference between

vehicle and drug treated dimer populations will be directly proportional to the vehicle dimer population (given a constant extent of drug binding) as shown in equation 16.

$$\text{Difference in dimer population} = F_{\text{bound}} D\%_{\text{vehicle}} \quad 16)$$

This is one possible explanation why in the presence of Ca^{2+} the observed impact of pimobendan on cTnC is reduced at every level of reconstitution, a trend which would otherwise elude reason. Tables 5 and 6 were generated by dividing the values reported for pimobendan in tables 3 and 4 by $D\%_{\text{vehicle}}$ for that reconstitution level. Thus, the values reported in tables 5 and 6 are the percent difference between the dimer populations of vehicle and pimobendan treated samples, and in the case where $D\%_{\text{drug}} = 0$ (which seems to be the case for pimobendan) this percent difference is equivalent to the fraction of pimobendan bound cTnC. Looking at tables 5 and 6 the familiar trends of increased sensitizer impact in the presence of Ca^{2+} and cTnI are seen. Thus, if the assumption that pimobendan bound cTnC exists with a fully open hydrophobic cleft nearly 100% of the time, then it can be concluded from the above reasoning that pimobendan binding to cTnC is enhanced by the presence of Ca^{2+} and/or cTnI. Other explanations may also account for these results, however more in depth structural studies involving pimobendan binding to cTnC are needed as there is a paucity of structural data for pimobendan bound cTnC.

Materials and Methods

Mutant generation, protein expression, and labeling

A recombinant double cysteine mutant of cTnC (cTnC(T13C/N51C)), as well as wild type cTnI (cTnI(wt)), wild type cTnT (cTnT(wt)), and a cTnT with phosphorylation mimicking glutamic acid at residue 204 (cTnT(T204E)) were generated from wild type rat protein clones using approaches similar to those previously reported.[16, 25–27] Briefly, using the GeneTailor™ Site-Directed Mutagenesis System (Invitrogen, Carlsbad, CA, USA), rat cDNA clones of wild-type cTnC, cTnI, and cTnT sub-cloned into the plasmid pSBETa were used as template DNA to generate cTnC(T13C/N51C), cTnI(wt), cTnT(wt), and cTnT(T204E). Note that cTnC(T13C/N51C)'s endogenous cysteines, Cys-35 and Cys-84, have each been substituted with serine. The regulatory function of $cTnC(13C/51C)_{TAMRA2}$, used before in our laboratory, was verified by testing its ability to participate in the Ca^{2+} dependent regulation of acto-S1 ATPase activity (data not shown). Recombinant cTnC, cTnI and cTnT clones were overexpressed in *E. coli* strain BL21(DE3) cells and purified as previously described.[18, 28–30]

Residues 13 and 51 in cTnC were chosen as labeling sites because they are not part of any alpha helices or Ca^{2+} coordination sites, thus labeling to these residues should have minimal impact on cTnC's function, while simultaneously affording the labeled molecules a high degree of mobility. Labeling of cTnC(T13C/N51C) with tetramethylrhodamine-5-maleimide (TAMRA, Setareh Biotech) was accomplished by eliminating the presence of reducing agent, in this case DTT, to facilitate exposure of the sulfhydryl groups in the cysteine residues. Subsequent incubation with 4–5 molar excess TAMRA overnight produced a

mixture of unlabeled, singly labeled and doubly labeled cTnC(T13C/N51C). Excess DTT was then added to terminate the labeling reaction. The labeling process was repeated once more to increase the abundance of double labeled cTnC(T13C/N51C). Chromatographic separation of unlabeled, single labeled, and double labeled cTnC(T13C/N51C) was carried out on a DEAE column. Resolution of the singly and doubly labeled protein was only partial and the final sample utilized for this study contained a small amount of singly labeled cTnC. In order to account for the effect of singly labeled cTnC(T13C/N51C) on our TAMRA monomer/dimer measurements knowledge of the labeling ratio was required (see Absorbance data processing for more details). The labeling ratio was determined by finding the total TAMRA concentration and dividing it by the cTnC(T13C/N51C) concentration. The TAMRA concentration was determined spectroscopically by dividing the deconvoluted TAMRA absorbances (see Absorbance data processing) at 554 nm and 520 nm by their respective extinction coefficients (ε_{554}= 66,100 $cm^{-1}M^{-1}$ and ε_{520}= 64,200 $cm^{-1}M^{-1}$) and adding these values together to obtain the total concentration of TAMRA present in the sample.[12] The concentration of cTnC(T13C/N51C) was determined by measuring the absorbance at 280 nm, adjusting this absorbance by a correction factor based on the total TAMRA concentration, and then dividing this adjusted absorbance by cTnC(T13C/N51C)'s extinction coefficient ε_{280}= 4,470 $cm^{-1}M^{-1}$ (via biomol.net's protein extinction coefficient tools). Correction factors for TAMRA absorbance at 280 nm were determined by serially diluting protein free TAMRA and recording its absorbance at 280 nm as a function of peak absorbance (either at 554 nm or 520 nm).

Reconstitutions

Doubly labeled cTnC(T13C/N51C) was reconstituted with 20% excess cTnI to yield the binary complex, or with 20% excess cTnI and cTnT to yield the ternary complex. Inclusion of 20% excess cTnI and cTnT was done to ensure all cTnC(T13C/N51C) was complexed.[18, 27, 31] Reconstitution was achieved by mixing proteins in the appropriate ratio and gradually reducing the concentration of urea from 6-0 M and KCl from 0.5–0.15 M via dialysis. This was followed by a final dialysis into titration buffer, which consists of 2 mM ethylene glycol-bis(β-aminoethyl ether)-N,N,N′,N′-tetraacetic acid (EGTA), 5 mM nitrilotriacetic acid (NTA), 50 mM 3-(*N*-morpholino)propanesulfonic acid (MOPS), 150 mM KCl, 5 mM MgCl2, and 1 mM dithiothreitol (DTT) at pH 7.10. Multiple experiments were performed on reconstituted samples within 5 days, and no protein degradation was observed by electrophoretic analysis over this time period.

Ca^{2+}-sensitizer preparation

The three Ca^{2+}-sensitizers used in this study levosimendan (Sigma-Aldrich), bepridil (Sigma-Aldrich) and pimobendan (Merck) were dissolved in enough dimethylformamide (DMF) to make 6 mM drug stock solutions. Stock solutions were kept at 4°C to prevent degradation and were remade every 2 weeks.

Absorbance spectra measurements

Absorbance spectra measurements were conducted at 22 °C on samples containing 1 μM $cTnC(13C/51C)_{TAMRA2}$, cTnI(wt)-$cTnC(13C/51C)_{TAMRA2}$, cTnI(wt)-$cTnC(13C/51C)_{TAMRA2}$-cTnT(wt), or cTnI-$cTnC(13C/51C)_{TAMRA2}$-cTnT(T204E) in titration buffer

containing 1.67% DMF by volume. Ca^{2+} free measurements were performed in Ca^{2+} free titration buffer, while Ca^{2+} saturated samples contained 10 mM Ca^{2+}. Drug samples contained 100 μM of their respective Ca^{2+}-sensitizer while control samples did not. Absorbance readings were obtained for the wavelength range 450–700 nm. All data was saved and exported to Excel for analysis. Extraction of the fractional abundance (relative to moles TAMRA) of monomer and dimer was performed as described in Absorbance spectra processing.

Absorbance data processing

The absorbance spectra of a mixed population of monomeric and dimeric TAMRA is a weighted average of the absorbance spectra of the pure monomer and pure dimer, with weights equal to the percent abundance of that species in solution. Thus, if one knows the spectra of the pure monomer and pure dimer the fraction of monomer and dimer in a mixed population can be obtained. Spectra for the pure monomer and dimer were obtained from the study by Christie et al., who created a high purity dimeric TAMRA species which dissociates into pure monomer in reducing conditions.[12] The absorbance spectrum of the pure dimer showed an extinction coefficient at 520 nm of 64,200 $cm^{-1}M^{-1}$ (relative to moles of TAMRA) with a 554nm/520nm ratio of 0.38, meaning that 38% of the absorbance at the dimer peak wavelength contributes to the absorbance at the monomer peak wavelength. The absorbance spectrum of pure monomer showed an extinction coefficient at 554 nm of 66,100 $cm^{-1}M^{-1}$ relative to moles TAMRA, with a 520nm/554nm of 0.42. The absorbance spectra collected in this study were deconvoluted using a method similar to that of West and Pearce.[32] First the peak intensity at 554 nm is assumed to arise entirely from monomeric TAMRA, $A_{554}M_1 = A_{554}$. This means that the contribution of monomer to the absorbance at 520 nm is $0.42A_{554}M_1$. This allows us to make an initial estimate of the absorbance at 520 nm arising from dimer, $A_{520}D_1 = A_{520} - 0.42A_{554}M_1$. This in turn allows us to update our estimate of the monomer contribution to absorbance at 554 nm, $A_{554}M_2 = A_{554} - 0.38A_{520}D_1$. Which allows us to update our estimate of the absorbance at 520 nm arising from dimer, $A_{520}D_2 = A_{520} - 0.42A_{554}M_2$. This process is repeated several more times until the values converge, thus giving us the absorbance at 554 nm arising from monomer and the absorbance at 520 nm arising from dimer. Dividing the deconvoluted monomer and dimer peak absorbances by their respective extinction coefficients (ε_{554}= 66,100 $cm^{-1}M^{-1}$ and ε_{520}= 64,200 $cm^{-1}M^{-1}$) yields the concentrations of monomeric and dimeric TAMRA in the sample. Finally, dividing the concentration of dimeric TAMRA by the total TAMRA concentration gives the fractional abundance of dimeric TAMRA. The presence of singly labeled cTnC(T13C/N51C) in these samples serves to reduce the apparent fractional abundance of dimeric TAMRA. This is because the singly labeled species is unable to participate in dimerization but gets included when determining the total concentration of TAMRA. This causes the fractional abundance of dimeric TAMRA species to appear less than it actually is. In order to adjust from the apparent to the true fractional abundance of dimer we need to multiply by the adjustment factor shown in equation 17 below, which removes single labeled cTnC's contribution from the total TAMRA concentration.

$$\text{Labeling Ratio Adjustment Factor} = \frac{\text{Labeling ratio}/2}{\text{Labeling ratio} - 1} \quad 17)$$

Statistical analysis

All data was analyzed via two-way ANOVA using GraphPad Prism 7.02, comparisons were made using TUKEY's honest significant difference ($p < 0.05$).

Acknowledgments

This work is supported by National Institutes of Health Grants R21 HL109693 (WJD), and American Heart Association grants 17GRNT33460153 (WJD).

References

1. Li MX, Hwang PM. Structure and function of cardiac troponin C (TNNC1): Implications for heart failure, cardiomyopathies, and troponin modulating drugs. Gene. 2015; 571(2):153–66. [PubMed: 26232335]
2. Schlecht W, Li KL, Hu D, Dong W. Fluorescence Based Characterization of Calcium Sensitizer Action on the Troponin Complex. Chem Biol Drug Des. 2016; 87(2):171–81. [PubMed: 26375298]
3. Schlecht W, Zhou Z, Li KL, Rieck D, Ouyang Y, Dong WJ. FRET study of the structural and kinetic effects of PKC phosphomimetic cardiac troponin T mutants on thin filament regulation. Arch Biochem Biophys. 2014; 550–551:1–11.
4. Endoh M. Cardiac Ca2+ signaling and Ca2+ sensitizers. Circ J. 2008; 72(12):1915–25. [PubMed: 18981594]
5. Li Y, Love ML, Putkey JA, Cohen C. Bepridil opens the regulatory N-terminal lobe of cardiac troponin C. Proc Natl Acad Sci U S A. 2000; 97(10):5140–5. [PubMed: 10792039]
6. He Y, Haque MM, Stuehr DJ, Lu HP. Single-molecule spectroscopy reveals how calmodulin activates NO synthase by controlling its conformational fluctuation dynamics. Proc Natl Acad Sci U S A. 2015; 112(38):11835–40. [PubMed: 26311846]
7. Lu HP. Single-molecule protein interaction conformational dynamics. Curr Pharm Biotechnol. 2009; 10(5):522–31. [PubMed: 19689321]
8. Cordina NM, Liew CK, Gell DA, Fajer PG, Mackay JP, Brown LJ. Effects of calcium binding and the hypertrophic cardiomyopathy A8V mutation on the dynamic equilibrium between closed and open conformations of the regulatory N-domain of isolated cardiac troponin C. Biochemistry. 2013; 52(11):1950–62. [PubMed: 23425245]
9. Robinson JM, Cheung HC, Dong W. The cardiac Ca2+-sensitive regulatory switch, a system in dynamic equilibrium. Biophys J. 2008; 95(10):4772–89. [PubMed: 18676638]
10. Pineda-Sanabria SE, Robertson IM, Sun YB, Irving M, Sykes BD. Probing the mechanism of cardiovascular drugs using a covalent levosimendan analog. J Mol Cell Cardiol. 2016; 92:174–84. [PubMed: 26853943]
11. Knowles AC, Irving M, Sun YB. Conformation of the troponin core complex in the thin filaments of skeletal muscle during relaxation and active contraction. J Mol Biol. 2012; 421(1):125–37. [PubMed: 22579625]
12. Christie RJ, Tadiello CJ, Chamberlain LM, Grainger DW. Optical properties and application of a reactive and bioreducible thiol-containing tetramethylrhodamine dimer. Bioconjug Chem. 2009; 20(3):476–80. [PubMed: 19249862]
13. Selwyn JE, Steinfeld JI. Aggregation of equilibriums of xanthene dyes. The Journal of Physical Chemistry. 1972; 76(5):762–774.

14. Hernando J, van der Schaaf M, van Dijk EMHP, Sauer M, García-Parajó MF, van Hulst NF. Excitonic Behavior of Rhodamine Dimers:] A Single-Molecule Study. The Journal of Physical Chemistry A. 2003; 107(1):43–52.
15. Ajtai K, Ilich PJK, Ringler A, Sedarous SS, Toft DJ, Burghardt TP. Stereospecific reaction of muscle fiber proteins with the 5′ or 6′ isomer of (iodoacetamido)tetramethylrhodamine. Biochemistry. 1992; 31(49):12431–12440. [PubMed: 1463729]
16. Dong WJ, Jayasundar JJ, An J, Xing J, Cheung HC. Effects of PKA phosphorylation of cardiac troponin I and strong crossbridge on conformational transitions of the N-domain of cardiac troponin C in regulated thin filaments. Biochemistry. 2007; 46(34):9752–61. [PubMed: 17676764]
17. Lehrer SS. The regulatory switch of the muscle thin filament: Ca2+ or myosin heads? J Muscle Res Cell Motil. 1994; 15(3):232–6. [PubMed: 7929789]
18. Robinson JM, Dong WJ, Xing J, Cheung HC. Switching of troponin I: Ca(2+) and myosin-induced activation of heart muscle. J Mol Biol. 2004; 340(2):295–305. [PubMed: 15201053]
19. Sumandea MP, Pyle WG, Kobayashi T, de Tombe PP, Solaro RJ. Identification of a functionally critical protein kinase C phosphorylation residue of cardiac troponin T. J Biol Chem. 2003; 278(37):35135–44. [PubMed: 12832403]
20. Veltri T, de Oliveira GA, Bienkiewicz EA, Palhano FL, Marques MA, Moraes AH, Silva JL, Sorenson MM, Pinto JR. Amide hydrogens reveal a temperature-dependent structural transition that enhances site-II Ca2+-binding affinity in a C-domain mutant of cardiac troponin C. Sci Rep. 2017; 7(1):691. [PubMed: 28386062]
21. Robertson IM, Pineda-Sanabria SE, Yan Z, Kampourakis T, Sun YB, Sykes BD, Irving M. Reversible Covalent Binding to Cardiac Troponin C by the Ca2+-Sensitizer Levosimendan. Biochemistry. 2016; 55(43):6032–6045. [PubMed: 27673371]
22. Li MX, Robertson IM, Sykes BD. Interaction of cardiac troponin with cardiotonic drugs: a structural perspective. Biochem Biophys Res Commun. 2008; 369(1):88–99. [PubMed: 18162171]
23. Wang X, Li MX, Sykes BD. Structure of the regulatory N-domain of human cardiac troponin C in complex with human cardiac troponin I147–163 and bepridil. J Biol Chem. 2002; 277(34):31124–33. [PubMed: 12060657]
24. Kleerekoper Q, Liu W, Choi D, Putkey JA. Identification of binding sites for bepridil and trifluoperazine on cardiac troponin C. J Biol Chem. 1998; 273(14):8153–60. [PubMed: 9525919]
25. Dong WJ, Robinson JM, Stagg S, Xing J, Cheung HC. Ca2+-induced conformational transition in the inhibitory and regulatory regions of cardiac troponin I. J Biol Chem. 2003; 278(10):8686–92. [PubMed: 12511564]
26. Xing J, Jayasundar JJ, Ouyang Y, Dong WJ. Forster resonance energy transfer structural kinetic studies of cardiac thin filament deactivation. J Biol Chem. 2009; 284(24):16432–41. [PubMed: 19369252]
27. Zhou Z, Li KL, Rieck D, Ouyang Y, Chandra M, Dong WJ. Structural dynamics of C-domain of cardiac troponin I protein in reconstituted thin filament. J Biol Chem. 2012; 287(10):7661–74. [PubMed: 22207765]
28. Dong WJ, Chandra M, Xing J, Solaro RJ, Cheung HC. Conformation of the N-terminal segment of a monocysteine mutant of troponin I from cardiac muscle. Biochemistry. 1997; 36(22):6745–53. [PubMed: 9184156]
29. Dong WJ, Xing J, Robinson JM, Cheung HC. Ca^{2+} induces an extended conformation of the inhibitory region of troponin I in cardiac muscle troponin. J Mol Biol. 2001; 314(1):51–61. [PubMed: 11724531]
30. Dong WJ, Xing J, Villain M, Hellinger M, Robinson JM, Chandra M, Solaro RJ, Umeda PK, Cheung HC. Conformation of the regulatory domain of cardiac muscle troponin C in its complex with cardiac troponin I. J Biol Chem. 1999; 274(44):31382–31390. [PubMed: 10531339]
31. Dong WJ, Xing J, Ouyang Y, An J, Cheung HC. Structural kinetics of cardiac troponin C mutants linked to familial hypertrophic and dilated cardiomyopathy in troponin complexes. J Biol Chem. 2008; 283(6):3424–32. [PubMed: 18063575]
32. West W, Pearce S. The Dimeric State of Cyanine Dyes. The Journal of Physical Chemistry. 1965; 69(6):1894–1903.

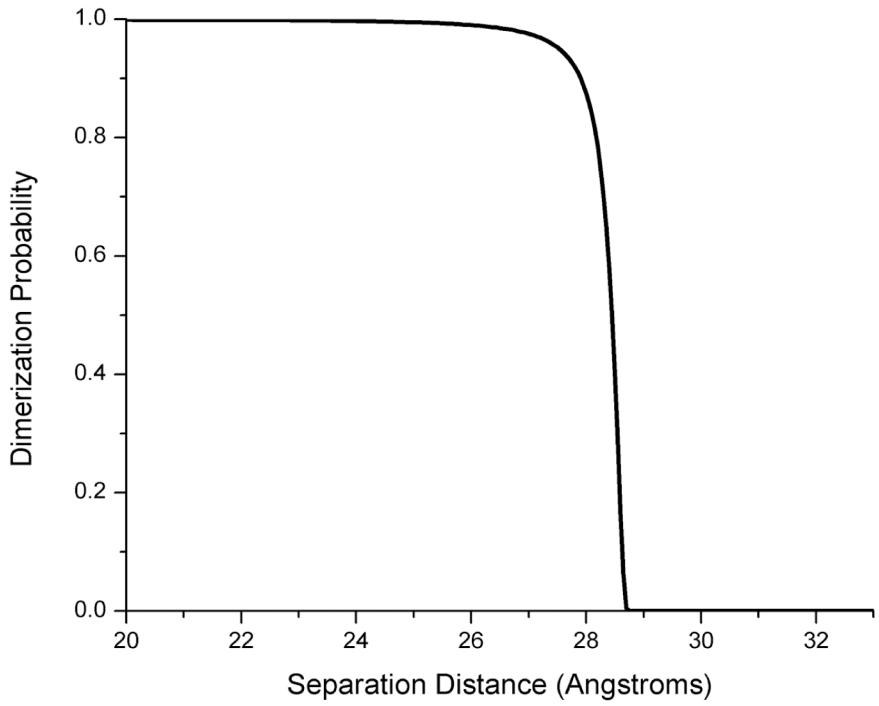

Figure 1.
The probability of dimerization as a function of 13C-51C separation distance according to the model developed in this study.

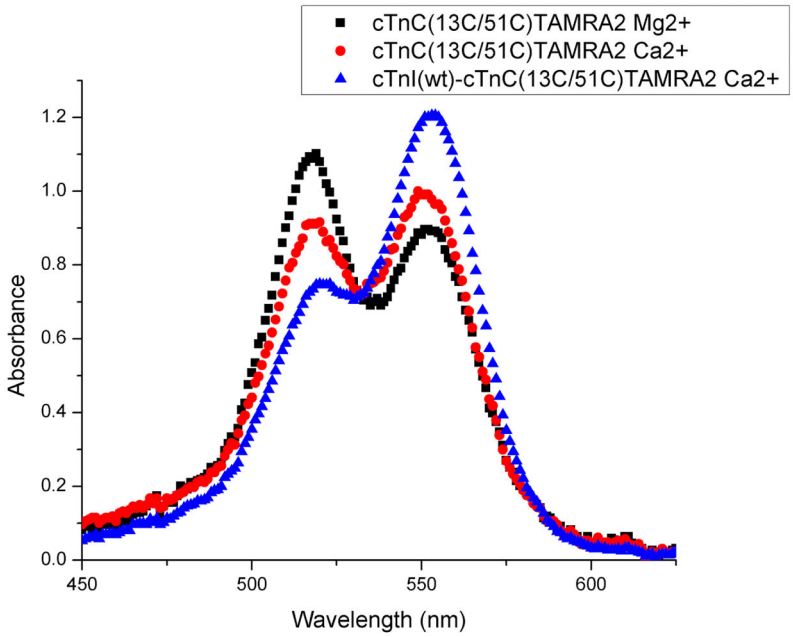

Figure 2.

Representative absorbance spectra collected from Mg^{2+}-cTnC(T13C/N51C)$_{TAMRA2}$ (dimeric TAMRA dominates), Ca^{2+}-cTnC(T13C/N51C)$_{TAMRA2}$ (dimeric and monomeric TAMRA nearly equal), and Ca^{2+}-cTnI(wt)-cTnC(T13C/N51C)$_{TAMRA2}$ (monomeric TAMRA dominates) illustrating how Ca^{2+} and cTnI influence the abundance of monomeric and dimeric TAMRA species which in turn alter the relative absorbance at 554 nm and 520 nm.

Table 1

Percentage of TAMRA population in the dimer state in the absence of Ca^{2+}.

Mg^{2+}-cTnC(T13C/N51C)$_{TAMRA2}$			
Vehicle *(N = 22)*	**Levosimendan *(N = 24)***	**Bepridil *(N = 24)***	**Pimobendan *(N = 8)***
85.5 ± 2.0[a]	85.1 ± 2.3	84.1 ± 1.6	57.8 ± 5.0*
Mg^{2+}-cTnI(wt)-cTnC(T13C/N51C)$_{TAMRA2}$			
Vehicle *(N = 25)*	**Levosimendan *(N = 24)***	**Bepridil *(N = 20)***	**Pimobendan *(N = 8)***
42.4 ± 3.1[b]	37.1 ± 5.7*	40.7 ± 2.7	26.0 ± 5.3*
Mg^{2+}-cTnI(wt)-cTnC(T13C/N51C)$_{TAMRA2}$-cTnT(wt)			
Vehicle *(N = 30)*	**Levosimendan *(N = 22)***	**Bepridil *(N = 19)***	**Pimobendan *(N = 8)***
54.7 ± 3.5[c]	50.8 ± 4.3*	52.9 ± 3.1	33.3 ± 2.3*
Mg^{2+}-cTnI(wt)-cTnC(T13C/N51C)$_{TAMRA2}$-cTnT(T204E)			
Vehicle *(N = 28)*	**Levosimendan *(N = 18)***	**Bepridil *(N = 20)***	**Pimobendan *(N = 9)***
56.5 ± 2.9[c]	51.0 ± 3.0*	53.7 ± 2.1	34.7 ± 4.1*
***P*-value**			
Reconstitution Level	**Sensitizer**	**R×S[t]**	
<0.001	<0.001	<0.001	

Values given as mean ± Std. Dev. Drug treated samples with an * superscript differ significantly from the vehicle control for that level of reconstitution and vehicle controls without a common letter superscript differ significantly ($P < 0.05$) as analyzed by two-way ANOVA and the TUKEY test. I, C T, and T(T204E) stand for cardiac troponins I, C, T and T(T204E) respectively, the abbreviations indicate which of the troponins are present at a given reconstitution level.

[t] R × S = Reconstitution Level × Sensitizer interaction effect.

Table 2

Percentage of TAMRA population in the dimer state in the presence of Ca^{2+}.

Ca^{2+}-cTnC(T13C/N51C)$_{TAMRA2}$			
Vehicle *(N = 22)*	**Levosimendan *(N = 23)***	**Bepridil *(N = 24)***	**Pimobendan *(N = 8)***
66.1 ± 2.4[a]	63.6 ± 3.6	64.1 ± 4.6	41.0 ± 3.1*
Ca^{2+}-cTnI(wt)-cTnC(T13C/N51C)$_{TAMRA2}$			
Vehicle *(N =25)*	**Levosimendan *(N = 24)***	**Bepridil *(N = 21)***	**Pimobendan *(N = 8)***
31.3 ± 3.9[b]	25.6 ± 5.2*	27.8 ± 4.8	15.4 ± 2.1*
Ca^{2+}-cTnI(wt)-cTnC(T13C/N51C)$_{TAMRA2}$-cTnT(wt)			
Vehicle *(N =30)*	**Levosimendan *(N = 22)***	**Bepridil *(N = 19)***	**Pimobendan *(N = 8)***
35.3 ± 5.8[b]	30.2 ± 6.0*	29.8 ± 7.9*	15.8 ± 4.2*
Ca^{2+}-cTnI(wt)-cTnC(T13C/N51C)$_{TAMRA2}$-cTnT(T204E)			
Vehicle *(N = 28)*	**Levosimendan *(N = 18)***	**Bepridil *(N = 20)***	**Pimobendan *(N = 9)***
35.2 ± 5.0[b]	30.6 ± 4.2	31.0 ± 5.9	19.7 ± 2.7*
***P*-value**			
Reconstitution Level	**Sensitizer**	**R×S[t]**	
<0.001	<0.001	<0.001	

Values given as mean ± Std. Dev. Drug treated samples with an * superscript differ significantly from the vehicle control for that level of reconstitution and vehicle controls without a common letter superscript differ significantly ($P < 0.05$) as analyzed by two-way ANOVA and the TUKEY test. I, C T, and T(T204E) stand for cardiac troponins I, C, T and T(T204E) respectively, the abbreviations indicate which of the troponins are present at a given reconstitution level.

[t] R × S = Reconstitution Level × Sensitizer interaction effect.

Table 3

Reduction in dimer population for each sensitizer treated sample compared to vehicle control at each level of reconstitution in the Mg^{2+} state.

Mg^{2+}-cTnC(T13C/N51C)$_{TAMRA2}$		
Levosimendan	**Bepridil**	**Pimobendan**
0.43	1.43	27.69
Mg^{2+}-cTnI(wt)-cTnC(T13C/N51C)$_{TAMRA2}$		
Levosimendan	**Bepridil**	**Pimobendan**
5.38	1.77	16.42
Mg^{2+}-cTnI(wt)-cTnC(T13C/N51C)$_{TAMRA2}$-cTnT(wt)		
Levosimendan	**Bepridil**	**Pimobendan**
3.90	1.80	21.34
Mg^{2+}-cTnI(wt)-cTnC(T13C/N51C)$_{TAMRA2}$-cTnT(T204E)		
Levosimendan	**Bepridil**	**Pimobendan**
5.46	2.80	21.80

Table 4

Reduction in dimer population for each sensitizer treated sample compared to vehicle control at each level of reconstitution in the Ca^{2+} state.

Ca^{2+}-cTnC(T13C/N51C)$_{TAMRA2}$		
Levosimendan	**Bepridil**	**Pimobendan**
2.47	2.03	25.09
Ca^{2+}-cTnI(wt)-cTnC(T13C/N51C)$_{TAMRA2}$		
Levosimendan	**Bepridil**	**Pimobendan**
5.71	3.51	15.8
Ca^{2+}-cTnI(wt)-cTnC(T13C/N51C)$_{TAMRA2}$-cTnT(wt)		
Levosimendan	**Bepridil**	**Pimobendan**
5.15	5.49	19.49
Ca^{2+}-cTnI(wt)-cTnC(T13C/N51C)$_{TAMRA2}$-cTnT(T204E)		
Levosimendan	**Bepridil**	**Pimobendan**
4.59	4.19	15.43

Table 5

Percent change in dimer population for pimobendan compared to vehicle control at each level of reconstitution in the Mg^{2+} state.

Mg^{2+}-cTnC(T13C/N51C)$_{TAMRA2}$
Pimobendan
32.37
Mg^{2+}-cTnI(wt)-cTnC(T13C/N51C)$_{TAMRA2}$
Pimobendan
38.69
Mg^{2+}-cTnI(wt)-cTnC(T13C/N51C)$_{TAMRA2}$-cTnT(wt)
Pimobendan
39.03
Mg^{2+}-cTnI(wt)-cTnC(T13C/N51C)$_{TAMRA2}$-cTnT(T204E)
Pimobendan
38.61

Table 6

Percent change in dimer population for pimobendan compared to vehicle control at each level of reconstitution in the Ca^{2+} state.

Ca^{2+}-cTnC(T13C/N51C)$_{TAMRA2}$
Pimobendan
37.96
Ca^{2+}-cTnI(wt)-cTnC(T13C/N51C)$_{TAMRA2}$
Pimobendan
50.54
Ca^{2+}-cTnI(wt)-cTnC(T13C/N51C)$_{TAMRA2}$-cTnT(wt)
Pimobendan
55.19
Ca^{2+}-cTnI(wt)-cTnC(T13C/N51C)$_{TAMRA2}$-cTnT(T204E)
Pimobendan
43.89